Dynamic response of marshes to perturbations in suspended sediment concentrations and rates of relative sea level rise

Dynamic response of marshes to perturbations in suspended sediment concentrations and rates of relative sea level rise

A. D'Alpaos,[1] S. M. Mudd,[2,3] and L. Carniello[4]

Received 18 May 2011; revised 5 September 2011; accepted 6 September 2011; published 12 November 2011.

[1] We have developed an analytical model of salt marsh evolution that captures the dynamic response of marshes to perturbations in suspended sediment concentrations, plant productivity, and the rate of relative sea level rise (RSLR). Sediment-rich and highly productive marshes will approach a new equilibrium state in response to a step change in the rate of RSLR faster than sediment-poor or less productive marshes. Microtidal marshes will respond more quickly to a step change in the rate of RSLR than mesotidal or macrotidal marshes. Marshes are more resilient to a decrease rather than to an increase in the rate of RSLR, and they are more resilient to a decrease rather than to an increase in sediment availability. Moreover, macrotidal marshes are more resilient to changes in the rate of RSLR than their microtidal counterparts. Finally, we find that a marsh's ability to record sea level fluctuations in its stratigraphy is fundamentally related to a timescale we call T_{FT}, or filling timescale, which is equal to the tidal amplitude divided by the maximum possible accretion rate on the marsh (a function of plant productivity, sediment properties, and availability). Marshes with a short-filling timescale (i.e., marshes with rapid sedimentation or small tidal amplitudes) are best suited to recording high-frequency fluctuations in RSLR, but our model suggests it is unlikely that marshes will be able to record fluctuations occurring over timescales that are shorter than decadal.

Citation: D'Alpaos, A., S. M. Mudd, and L. Carniello (2011), Dynamic response of marshes to perturbations in suspended sediment concentrations and rates of relative sea level rise, *J. Geophys. Res.*, *116*, F04020, doi:10.1029/2011JF002093.

1. Introduction

[2] Salt marshes are crucially important ecosystems because they buffer coastlines against storms [e.g., *Howes et al.*, 2010], filter nutrients and pollutants from tidal waters [e.g., *Costanza et al.*, 1997; *Larsen et al.*, 2010], provide nursery areas for coastal biota [e.g., *Perillo et al.*, 2009], and serve as a sink for organic carbon [e.g., *Chmura et al.*, 2003]. Marsh plants interact with sedimentation and the rate of relative sea level rise (RSLR); their combined effects determine the depth below mean high tide (MHT) of the marsh surface which in turn determines the productivity of marsh vegetation [e.g., *Morris et al.*, 2002]. Marsh productivity then feeds back on sedimentation rates because plants control sediment trapping efficiency [e.g., *Li and Yang*, 2009; *Mudd et al.*, 2010] and organic matter accumulation [*Nyman et al.*, 2006; *Neubauer*, 2008; *Mudd et al.*, 2009]. These feedbacks allow, under the right conditions, marshes to accrete at a pace equal to the rate of RSLR and thus maintain their position within the tidal frame despite rising sea levels. Recent studies of salt marsh ecosystems have shown, however, that if the rate of RSLR exceeds a threshold value, the plants on the marsh will drown [e.g., *Morris et al.*, 2002; *Marani et al.*, 2007, 2010; *Kirwan et al.*, 2010; *D'Alpaos*, 2011]. Marshes may also drown if sediment availability is reduced beyond a given value, thus preventing the marsh from keeping pace with current rates of RLSR [e.g., *Kirwan et al.*, 2010; *Marani et al.*, 2010; *D'Alpaos*, 2011]. Rising sea levels and the paucity of available sediment are in fact dominant factors controlling drowning and consequent disappearance of marshes worldwide [e.g., *Day et al.*, 2000; *Blum and Roberts*, 2009; *Mudd*, 2011]. Once marsh macrophytes drown, the previously vegetated marsh will convert to mudflats at an elevation much lower than the former marsh [*Fagherazzi et al.*, 2006; *Marani et al.*, 2007, 2010]. To predict this threshold and to explore the ecomorphodynamic evolution of salt marsh ecosystems, a number of numerical models have been developed over the last few decades [e.g., *Allen*, 1990; *French*, 1993; *Morris et al.*, 2002; *Rybczyk and Cahoon*, 2002; *Temmerman et al.*, 2003; *D'Alpaos et al.*, 2006, 2007; *Kirwan and Murray*, 2007; *Marani et al.*, 2007; *Mudd et al.*, 2009; *Larsen and Harvey*, 2010]. One drawback of these models, however, is that a large number of time consuming model runs are required to, for example, determine the functional relationship between suspended sediment concentration (SSC) and marsh stability [e.g., *Kirwan et al.*, 2010]. In this contribution we develop an analytical model capable of predicting salt marsh response to environmental forcings. While lacking the complexity of existing numerical models, our parsimonious analytical model

[1]Department of Geosciences, University of Padova, Padua, Italy.
[2]School of GeoSciences, University of Edinburgh, Edinburgh, UK.
[3]Also at Earth Research Institute, University of California, Santa Barbara, California, USA.
[4]Department IMAGE, University of Padova, Padua, Italy.

0148-0227/11/2011JF002093

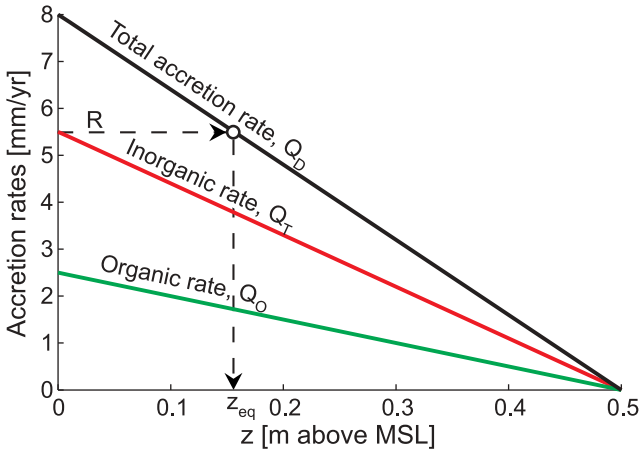

Figure 1. Organic, inorganic, and total accretion rates as functions of marsh elevation above mean sea level (MSL). The marsh is forced by a semidiurnal tide with amplitude H = 0.5 m and is characterized by an SSC, C_0 = 20 mg L^{-1}, leading to a maximum inorganic deposition rate α_T = 5.5 mm yr^{-1} (obtained by solving the sediment balance equation in the water column when ρ_s = 2600 kg m^{-3}, λ = 0.5, and $w_s = 2 \times 10^{-4}$ m s^{-1}) [*Marani et al.*, 2007]. The maximum organic rate is γ_0 = 2.5 mm yr^{-1}, whereas the maximum total accretion rate is k = 8.0 mm yr^{-1}. The equilibrium elevation corresponding to a rate of RSLR of 5.5 mm yr^{-1} is also shown.

allows instant assessment of key dynamical behavior of salt marsh surfaces such as the response timescale of these surfaces to perturbation and their stability in the face of changing SSCs and rates of RSLR.

2. Analytical Model

[3] Vegetation on marsh platforms typically occupies elevations between mean sea level (MSL) and MHT [*McKee and Patrick*, 1988; *Kirwan and Guntenspergen*, 2010]. We consider a marsh platform, whose elevation, z, is computed with respect to the local MSL (i.e., z is a moving coordinate with z = 0 at MSL; if ζ is an absolute elevation then $z = \zeta -$ MSL). The marsh platform is subjected to a sinusoidal tide of period T_{tide} and amplitude H (i.e., $z = H$ at MHT) and is populated by a single vegetation species, namely *Spartina alterniflora*. The time evolution of the marsh-platform elevation, z, is described by the annually averaged sediment balance equation for the marsh surface

$$\frac{dz}{dt} = Q_D - Q_E - R \tag{1}$$

where Q_D is the deposition rate, Q_E is the erosion rate, and R is the rate of RSLR; that is, sea level variations plus local subsidence. It is worthwhile noting that the term R is introduced because the elevation, z, is computed with respect to MSL (z is relative to a moving tidal frame). We have introduced some simplifying assumptions in order to maintain analytical tractability:

[4] 1. The deposition rate is generally modeled as the sum of the settling (Q_S), particle capture on plant stems and leaves (Q_C), and organic deposition rates (Q_O). Here we consider the role of organic production and inorganic deposition, the latter being modeled as the sum of settling and particle capture. This assumption is consistent with recent findings of *Marani et al.* [2010] and *Mudd et al.* [2010] who showed that capture is significantly smaller than settling for flow velocities commonly observed in tidal marshes (up to 5 cm s^{-1}). Moreover, these authors demonstrated that for a given elevation of the vegetated platform, settling decreases as capture increases and vice versa, so that the total inorganic deposition flux ($Q_T = Q_S + Q_C$, the subscript T denoting trapping; that is, the sum of particle settling and capture on plant stems) remains nearly constant.

[5] 2. We also neglect erosion fluxes over the marsh platform (i.e., Q_E = 0) possibly owing to tidal currents and wind waves. Such assumption is based on the observations that (1) tidal currents are generally too weak to erode the vegetated marsh surface and (2) wind-wave erosion is negligible because of the combined effect of the reduced water depth over the platform, which limits the wind-induced bottom shear stress [e.g., *Christiansen et al.*, 2000; *Carniello et al.*, 2005], and the presence of halophytes, which both damp waves [*Möller et al.*, 1999; *Augustin et al.*, 2009] and protect the surface against erosion by currents [*Neumeier and Ciavola*, 2004].

[6] 3. We express Q_D as a linearly decreasing function of marsh elevation between MSL (z = 0) and MHT ($z = H$)

$$Q_D(z) = \alpha_T\left(1 - \frac{z}{H}\right) + \gamma_O\left(1 - \frac{z}{H}\right), \tag{2}$$

where the first and the second term on the right-hand side of equation (2) represent the inorganic deposition rate (i.e., settling plus particle capture), Q_T, and the organic rate, Q_O, respectively (Figure 1), for a *Spartina*-dominated marsh. The parameters α_T and γ_O are the maximum inorganic and organic deposition rates, respectively, and, for a given tidal amplitude, determine how rapidly Q_T and Q_O decrease with z (Figure 1). The linear decrease in Q_T with z has also been assumed in recent models of marsh evolution [*Morris et al.*, 2002; *Kirwan and Murray*, 2007]. *Marani et al.* [2007, 2010] demonstrated the validity of this assumption by numerically integrating a physically based settling model over a tidal cycle for the range of intertidal elevations.

[7] Following *Marani et al.* [2007, 2010], we calculate α_T by numerically solving a sediment balance equation in the water column [e.g., *Krone*, 1987; *Temmerman et al.*, 2003; *Marani et al.*, 2007]:

$$\frac{d(DC)}{dt} = -w_s \cdot C + \tilde{C} \cdot \frac{dh}{dt}, \tag{3}$$

with

$$\widetilde{C}(z,t) = \begin{cases} C_0 & when \quad \frac{dh}{dt} > 0 \\ C(z,t) & when \quad \frac{dh}{dt} < 0 \end{cases}, \tag{4}$$

where $D(t) = h(t)$-z is the instantaneous water depth; $h(t)$ is the instantaneous tidal elevation with respect to the current MSL; $C(z, t)$ is the depth-averaged instantaneous SSC; and w_s is the settling velocity, which can be estimated on the basis of sediment size (e.g., for d_{50} = 50 μm,

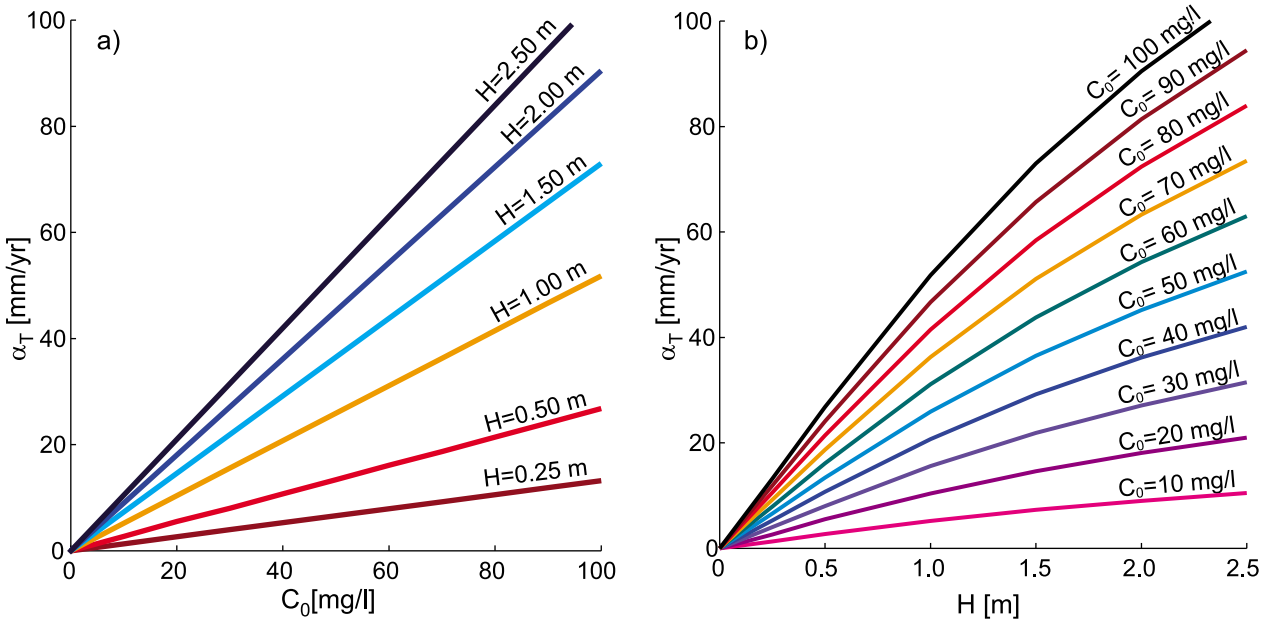

Figure 2. Values of α_T obtained by solving the sediment balance equation in the water column for different values of the forcing SSC, C_0, and of the tidal amplitude, H (when a tidal period T_{tide} = 12 h, a settling velocity $w_s = 2 \times 10^{-4}$ m s^{-1}, a porosity $\lambda = 0.5$, and a sediment density $\rho_s = 2600$ kg m^{-3} are assumed). (a) The α_T values as a function of the forcing SSC, C_0, for different tidal amplitudes. (b) The α_T values as a function of the tidal amplitude for different C_0 values. We note that α_T is a function of the tidal amplitude, H, the forcing SSC, C_0, the settling velocity, w_s, and the bulk density ρ_b: $\alpha_T = f(w_s, C_0, \rho_b, H)$. In particular, α_T linearly increases with w_s and C_0, linearly decreases (inversely related) with ρ_b, and increases nonlinearly with H. For reference, and for the parameter values above recalled, we evaluate $\alpha_T = f_1(H) \times C_0$, where $f_1(H)$ = 0.132, 0.268, 0.518, 0.730, 0.905, and 1.050 for H = 0.25, 0.5, 1.0, 1.5, 2.0, and 2.5 m, respectively (note that when C_0 is expressed in milligrams per liter, α_T is expressed in millimeters per year).

w_s = 0.2 mm s^{-1}). The first term on the right-hand side of equation (3) is the instantaneous inorganic flux (Q_T), while the second term represents the exchange of sediment between the platform and its surrounding: when the flow is toward the platform it carries a fixed concentration, C_0, representing the forcing sediment supply (e.g., from the adjacent channels or tidal flats), and therefore $\tilde{C}(z, t) = C_0$. When the flow drains the platform (i.e., during the ebb tide), the outgoing concentration is the instantaneous concentration, and in this case $\tilde{C}(z, t) = C(z, t)$. The solution of equation (3) yields the instantaneous values of the depth-averaged SSC from which one can determine the annually averaged sediment inorganic flux

$$Q_T(z) = \frac{w_s n_T}{\rho_b T_{\text{tide}}} \int_{T_{\text{tide}}} C(z,t)dt, \tag{5}$$

where T_{tide} is the tidal period, n_T is the number of tidal periods in a year, and $\rho_b = \rho_s(\lambda - 1)$ is the bulk density, with ρ_s = 2650 kg m^{-3} and the porosity $\lambda = 0.5$, which implicitly accounts for the result of compaction processes. Figure 1 shows the linear decrease of the total inorganic flux, Q_T (in red), with marsh elevation, computed on the basis of the point model which solves a sediment continuity equation for the water column [*Marani et al.*, 2007, 2010] in the case of a *Spartina*-dominated marsh. Q_T is maximum when z = 0 ($Q_T = \alpha_T$ at MSL) and it linearly decreases to vanish when $z = H$. Figure 2 shows α_T values obtained by solving equation (3), for different values of the forcing SSC, C_0, and of the tidal amplitude, H (see also Table 1). For a prescribed tidal amplitude, α_T linearly increases with the forcing SSC (Figure 2a), whereas for a given value of the forcing SSC, α_T increases less than linearly with the tidal amplitude (Figure 2b).

[8] The linear decrease of Q_O with z (Figure 1) is justified by assuming Q_O proportional to the annually averaged aboveground plant dry biomass [*Randerson*, 1979] and by expressing *Spartina* biomass as a linearly decreasing function of z between MSL and MHT, as suggested by *Mudd et al.* [2004] to approximate the biomass-elevation relationship originally measured by *Morris et al.* [2002] in *Spartina*-dominated marshes. The parameter γ_O depends on vegetation characteristics such as rates of root growth and decomposition rates [e.g., *Mudd et al.*, 2009]. Figure 1 shows the linear decrease of the organic flux, Q_O (in green), with marsh elevation, and also illustrates the relationship of the total sediment deposition, Q_D, to elevation, z.

[9] On the basis of the above assumptions equation (1) becomes a first-order linear differential equation

$$\frac{dz}{dt} = -\frac{k}{H}z + k - R \tag{6}$$

where $k = \alpha_T + \gamma_O$ is the maximum total accretion rate over the marsh platform. Equation (6) can be used to examine the

Table 1. Values of α_T Obtained by Solving a Sediment Balance Equation in the Water Column for Different Values of the Forcing SSC, C_0, and of the Tidal Amplitude, H[a]

C_0 (mg L^{-1})	H = 0.25 m (mm yr^{-1})	H = 0.50 m (mm yr^{-1})	H = 1.00 m (mm yr^{-1})	H = 1.50 m (mm yr^{-1})	H = 2.00 m (mm yr^{-1})	H = 2.50 m (mm yr^{-1})
10	1.3	2.7	5.2	7.3	9.0	10.5
20	2.6	5.5	10.4	14.6	18.1	21.0
30	4.0	8.0	15.6	21.9	27.1	31.5
40	5.3	10.7	20.7	29.2	36.2	42.0
50	6.6	13.4	25.9	36.5	45.2	52.5
60	7.9	16.1	31.1	43.8	54.3	63.0
70	9.2	18.7	36.3	51.1	63.3	75.5
80	10.6	21.4	41.5	58.4	72.4	84.0
90	11.9	24.1	46.7	65.7	81.4	94.5
100	13.2	26.8	51.8	73.0	90.5	105.5

[a]See *Marani et al.* [2007]. A tidal period T_{tide} = 12 h, a settling velocity $w_s = 2 \times 10^{-4}$ m s^{-1}, a porosity $\lambda = 0.5$, and a sediment density $\rho_s = 2600$ kg m^{-3} were assumed.

evolution of a marsh surface in response to changes in either the rate of RSLR or changes in the SSC.

3. Results

3.1. Marsh Response to a Step Change in the Rate of Relative Sea Level Rise

[10] First, we explore the case of a constant rate of RSLR. The equilibrium elevation of the marsh surface, z_{eq}, can be obtained by setting $dz/dt = 0$ in equation (6) (i.e., when marsh accretion, Q_D, matches the rate of RSLR, R; see also Figure 1):

$$z_{eq} = H\left(1 - \frac{R}{k}\right) \tag{7}$$

For a fixed tidal amplitude, H, and a given value of k (depending on the forcing SSC, C_0, and vegetation productivity) the equilibrium elevation, z_{eq}, decreases as the rate of RSLR, R, increases (Figure 1). However, the maximum rate of RSLR that the marsh can tolerate is equal to k; for values of R larger than k the marsh will drown ($z < 0$; i.e., the marsh surface is lower than MSL) and transition to a tidal flat. Figure 3 shows the equilibrium marsh elevations in the tidal frame (equilibrium elevations through normalization by tidal amplitude) as a function of the imposed rate of RSLR and sediment supply, for three different values of the tidal amplitude, thus allowing one to analyze marsh equilibria in different tidal settings (e.g., microtidal, mesotidal, and macrotidal). Equation (7) thus allows us to analytically determine the resilience of the marsh to RSLR rates (Figures 3a–3c) as function of both tidal amplitude, H, and k (which is a function of H and SSC, for a given value of the maximum organic accretion rate, γ_O). It clearly emerges that for a given suspended sediment concentration, the threshold rate of RSLR that results in drowning (i.e., $z \leq 0$) is greater in marshes with greater tidal amplitudes. Thus equation (7) compactly describes behavior that has been suggested by numerical modeling studies [e.g., *Allen*, 1995; *Kirwan et al.*, 2010]. For a given equilibrium elevation, z_{eq}, resulting from imposed rates of RSLR and sediment supply in different tidal settings, equation (2) allows us to determine the ratio between organic accretion, Q_O, and total deposition rate, Q_D (Figures 3d–3f). We never obtain a silty peat or peat marsh sensu *Allen* [1995], who predicted that organic production continues, and in fact continues at its highest productivity, when the marsh's elevation is greater than MHT. Such behavior is typical of Mediterranean tidal environments [e.g., *Day et al.*, 1999; *Marani et al.*, 2004; *Silvestri et al.*, 2005] or of sites in northern Europe. Our model, in contrast, follows the measurements of *Morris et al.* [2002] indicating a reduction in marsh marcrophyte productivity at elevations greater than MHT.

[11] We can also solve equation (6) to explore the evolution of a marsh through time if the rate of RSLR experiences a step change:

$$z(t) = z_{eq} + \left(z_0 - z_{eq}\right)e^{-\frac{k}{H}t} \tag{8}$$

$$Q_D(t) = R - \frac{k}{H}\left[z_0 - z_{eq}\right]e^{-\frac{k}{H}t} \tag{9}$$

where $z_0 = (1 - R_0/k_0)H$ is the initial marsh elevation in equilibrium with an initial rate of RSLR, R_0, and initial conditions for sediment load and vegetation productivity, k_0. The marsh will then evolve to an equilibrium elevation, z_{eq}, that reflects the new rate of RSLR (Figure 4). An equilibrium marsh elevation is one in which the marsh's position in the tidal frame does not change in time: at equilibrium the marsh accretion rate equals the new rate of RSLR. It is worthwhile noting that the equilibrium elevation is independent of the initial elevation and can be reached only asymptotically when $Q_D \rightarrow R$ for $t \rightarrow \infty$ (Figure 4). Moreover, Figure 4 makes it possible to analyze the case in which marshes characterized by a given sediment availability and vegetation productivity, in equilibrium with different initial R_0 values (i.e., $z_0 = (1 - R_0/k_0)H$), experience a step change in the rate of RSLR to R (with $k_0 = k$). It also allows analysis of cases in which marshes in equilibrium with a steady rate of RSLR (i.e., $z_0 = (1 - R_0/k_0)H$, with $R_0 = R$) evolve toward a new equilibrium elevation because of changes in the SSC or vegetation productivity (thus leading to changes in $k \neq k_0$).

[12] Equations (8) and (9) allow quantification of the timescale over which marshes respond to changes in the external forcing. We are able to quantify the time it takes for the marsh's total accretion rate, Q_D, to reach within 5% of the rate of RSLR after a change in forcings (i.e., rate of RSLR, sediment supply, or vegetation productivity). That is,

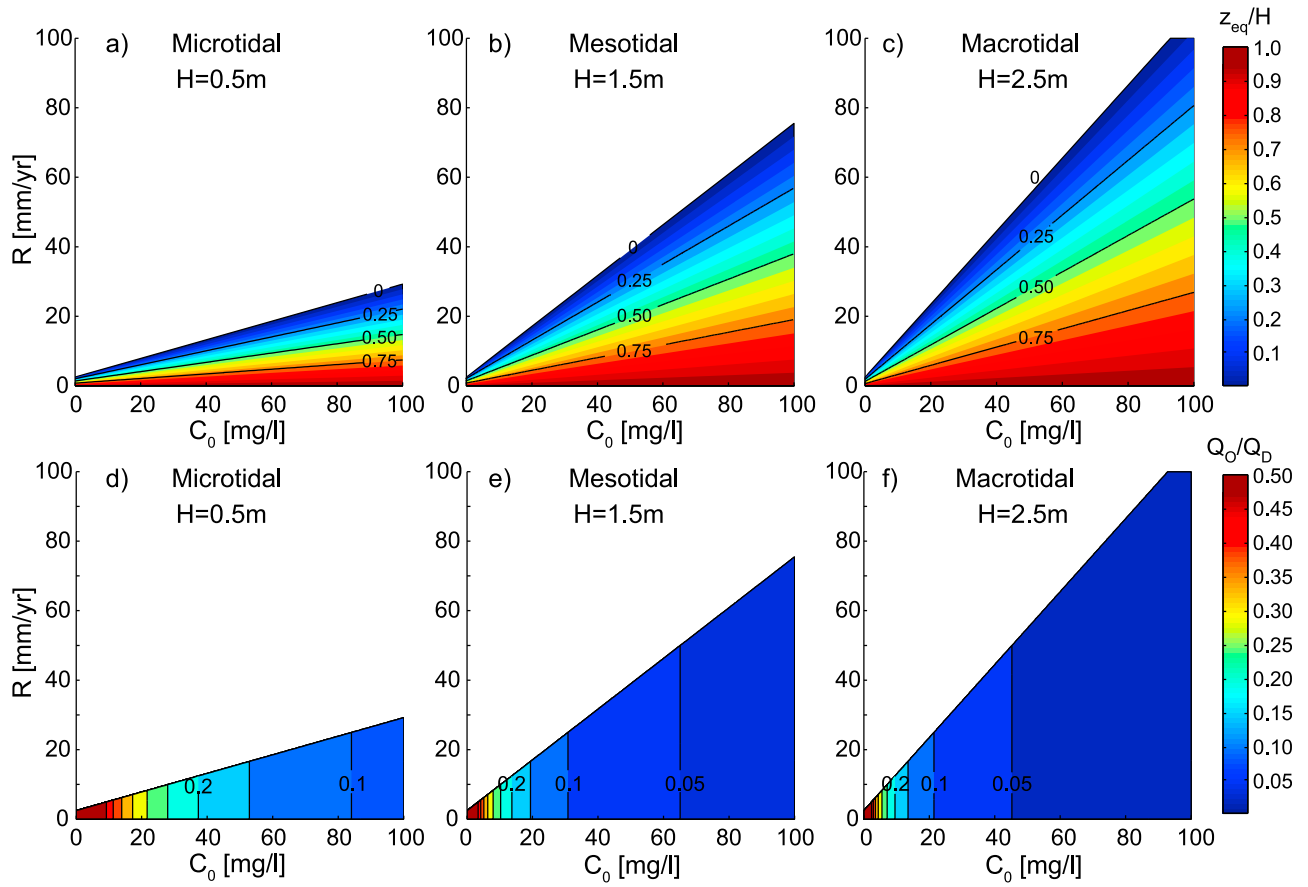

Figure 3. (a–c) Contour plots of the equilibrium elevation of the marsh surface divided by the tidal amplitude (z_{eq}/H) as a function of the rate of RSLR and forcing SSC, C_0, for microtidal (H = 0.5 m in Figure 3a), mesotidal (H = 1.5 m in Figure 3b), and macrotidal marshes (H = 2.5 m in Figure 3c). Uncolored areas represent drowned marshes. (d–f) Contour plots of the ratio between the organic accumulation rates and total accretion rates (Q_O/Q_D) as a function of SSC and the rate of RSLR for microtidal (Figure 3d), mesotidal (Figure 3e), and macrotidal marshes (Figure 3e).

we solve equation (9) such that $|Q_D - R| = 0.05R$ which, in the case of a step change to a new constant rate of RSLR, is

$$\tau_{CR} = -\frac{H}{k}\ln\left|\frac{0.05R}{k(1 - z_0/H) - R}\right|, \qquad (10)$$

where τ_{CR} (the subscript CR denotes constant rate) is the response timescale if the rate of RSLR is constant after the perturbation. This can be written as

$$\tau_{CR} = -\frac{H}{k}\ln\left|\frac{0.05R}{R_0 - R}\right| = -\frac{H}{k}\ln\left|\frac{0.05k_0}{k_0 - k}\right| \qquad (11)$$

to facilitate analysis of the response of marshes to changes in the rate of RSLR or SSC and vegetation productivity. For a fixed tidal amplitude, the response timescale decreases as SSC or organic production increase: sediment rich or highly productive marshes respond faster to environmental perturbation. This effect is more pronounced for greater tidal amplitudes (Figure 5a). For fixed sediment availability and vegetation productivity (i.e., fixed values of k), the response timescale increases as H increases (Figure 5b) and the increase is stronger if there is less suspended sediment. Note that as H increases k also increases, although k primarily increases with increasing SSC; see Table 1 and Figure 2.

[13] For fixed k and H values, Figure 6 shows the response timescale, τ_{CR}, as a function of R for different initial rates of RSLR, R_0. In the case of a step increase in the rate of RSRL, τ_{CR} mildly increases with the magnitude of the increase (e.g., for R_0 = 2 mm yr^{-1}, the time lag required to match newly imposed rates, R = 4, 6, and 8 mm yr^{-1} is equal to 144, 162, and 169 years, respectively) and depends on the initial rate of RSLR (e.g., for R_0 = 4 mm yr^{-1}, τ_{CR} = 119 and 144 years when the newly imposed R values are equal to 6 and 8 mm yr^{-1}, respectively). In the case of a step decrease in R, time lags strongly increase with the magnitude of the decrease (e.g., for R_0 = 6 mm yr^{-1}, the time required to match newly imposed rates, R = 3, 2, and 1 mm yr^{-1} is equal to 187, 231, and 288 years, respectively) and also depend on the initial rate R_0 (for R_0 = 4 mm yr^{-1}, τ_{CR} = 119, 187, and 226 years when the newly imposed rates, R, are equal to 3, 2, and 1 mm yr^{-1}, respectively). In other words, marshes that experience a step increase in the rate of

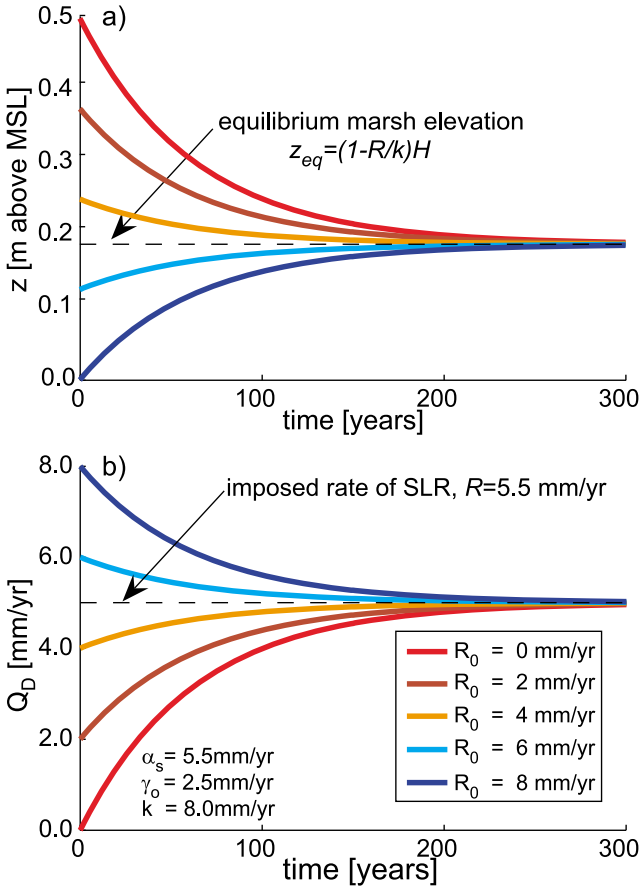

Figure 4. (a) Marsh elevations and (b) related total deposition rates characterizing the evolution of the platform toward equilibrium conditions starting from different initial elevations. The marsh is forced by a semidiurnal tide with amplitude $H = 0.5$ m and is characterized by an SSC, $C_0 = 20$ mg L^{-1}, leading to $\alpha_s = 5.5$ mm yr^{-1} and $k = 8.0$ mm yr^{-1} when $\gamma_0 = 2.5$ mm yr^{-1}. The imposed rate of RSLR is $R = 5.5$ mm yr^{-1}; the initial elevations, z_0, are in equilibrium with different initial R_0 values $R_0 = 0$, 2, 4, 6, and 8 mm yr^{-1} (with $k_0 = k = 8.0$ mm yr^{-1}).

RSLR equilibrate more rapidly than those that experience a step decrease in the rate of RSLR of the same magnitude.

3.2. Marsh Response to a Step Change in Sediment Availability

[14] Equation (11) allows us also to examine how the marsh responds to changes in sedimentation processes (e.g., increased SSC or vegetation productivity) if the rate of RSLR stays constant (Figure 7). When the SSC or/and vegetation productivity increase ($k > k_0$) shorter times are required to match a new equilibrium configuration than in the case of a decrease (of the same amount). For $k_0 = 10.5$ mm yr^{-1}, it takes about 70 years to match new equilibrium conditions forced with a value of $k = 15$ mm yr^{-1}, whereas it takes 230 years for marsh elevations to adjust to a decreased value of $k = 5$ mm yr^{-1}; for $k_0 = 5.2$ mm yr^{-1}, it takes about 145 years to match new conditions in equilibrium with $k = 7.5$ mm yr^{-1}, whereas it takes more than 470 years to adjust to $k = 2.5$ mm yr^{-1}.

3.3. Marsh Response to Sinusoidal Variations in the Rate of Relative Sea Level Rise

[15] We may also examine the case in which the rate of RSLR varies sinusoidally (i.e., $R(t) = R_1 + R_2 \sin \omega t$ where R_1 is a constant mean rate of RSLR around which oscillations occur), R_2 is the amplitude of the oscillation (which is equivalent to the maximum rate of change of the fluctuating component of relative MSL), ω is the angular frequency of the oscillation, equal to $(2\pi)/T$, and T is the period of the oscillation (Figure 8). In this case marsh elevation $z(t)$ and the accretion rate $Q_D(t)$ read

$$z(t) = \bar{z}_{eq} + \left(z_0 - \bar{z}_{eq} - \frac{R_2\omega}{(k/H)^2+\omega^2}\right)e^{-\frac{k}{H}t} - \frac{R_2}{(k/H)^2+\omega^2}\left(\frac{k}{H}\sin\omega t - \omega\cos\omega t\right) \quad (12)$$

$$Q_D(t) = R_1 - \frac{k}{H}\left(z_0 - \bar{z}_{eq} - \frac{R_2\omega}{(k/H)^2+\omega^2}\right)e^{-\frac{k}{H}t} + \frac{(k/H)R_2}{(k/H)^2+\omega^2}\left(\frac{k}{H}\sin\omega t - \omega\cos\omega t\right) \quad (13)$$

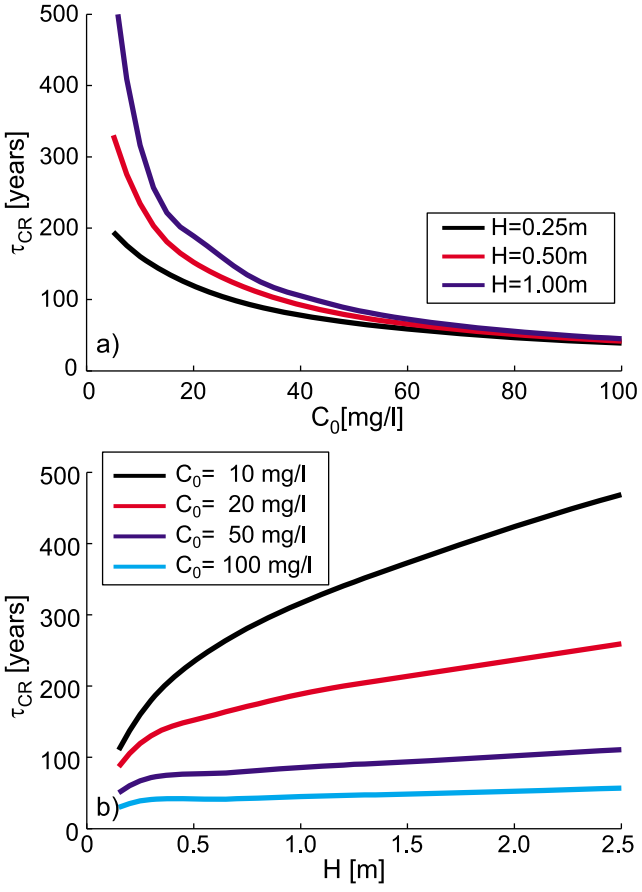

Figure 5. (a) Time lags, τ_{CR}, as a function of the SSC, C_0, computed for different tidal amplitudes, H (see equation (10)). (b) Time lags, τ_{CR}, as a function of H for different C_0 values. For both Figures 5a and 5b, $\gamma_0 = 2.5$ mm yr^{-1}, $R_0 = 3.0$ mm yr^{-1}, and $R = 5.0$ mm yr^{-1}.

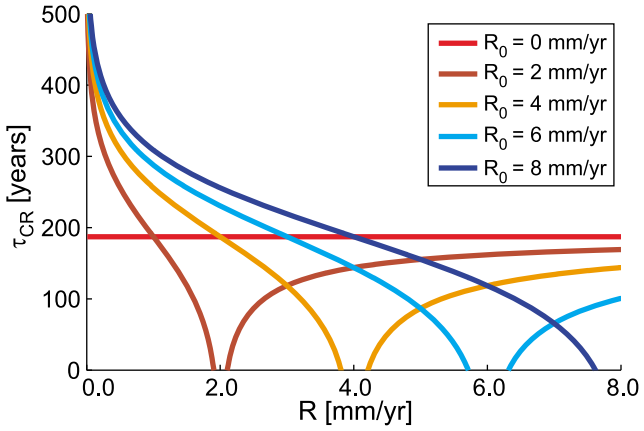

Figure 6. Time lags, τ_{CR}, as a function of the imposed value of R computed for different initial rates of RSLR, R_0, for k = 8.0 mm yr^{-1} and H = 0.5 m. Note that the time lag is independent of the imposed rate of RSLR, R, when the initial rate of RSLR, R_0, is null, as it emerges from equation (11). This result, directly emerging from the analytical solution of the theoretical framework proposed herein, deserves to be further investigated and tested against observational evidence.

where the first term on the right-hand side of equation (12), $\bar{z}_{eq} = (1-R_1/k)H$, is the average elevation around which time-dependent elevations oscillate (Figures 9a–9c), the second is the transient term, and the third describes the oscillation of marsh elevations around the average elevation. Analogous considerations hold for the terms on the right-hand side of equation (13): the first term, R_1, is the average total accretion rate around which oscillations in the total accretion rate occur (third term), as shown in Figures 9d–9f. We find that maximum and minimum values of Q_D correspond to points at which Q_D equals R, and that those points are equilibrium states (Figures 9d–9f). At equilibrium $dz/dt = 0$ and $Q_D = R$ from equation (1). However, because Q_D is a linear function of z (see equation (2)), Q_D is maximum or minimum when $dz/dt = 0$. It is worthwhile noting that the total accretion rate, Q_D, oscillates around the average accretion rate, R_1, with a reduced amplitude compared to that of the oscillating rate of RSLR, R_2 (Figures 9d–9f). Furthermore a lag (which we call τ_{SR}; the subscript SR denotes sinusoidal rate) is observed between maximum accretion rates and maximum rates of RSLR (Figures 9d–9f), which, in the case of a sinusoidal rate of RSLR, reads

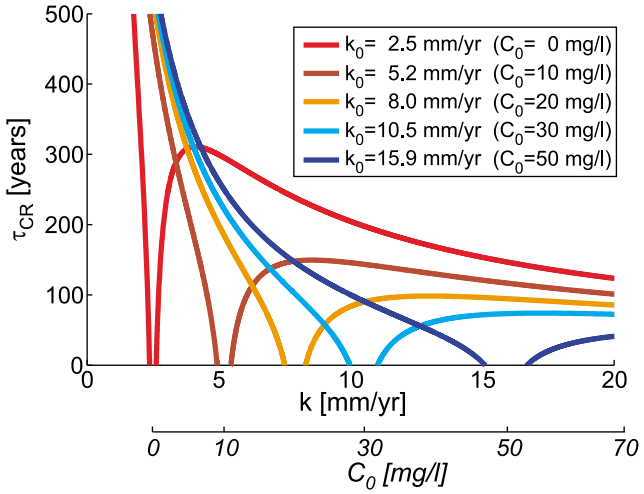

Figure 7. Time lags, τ_{CR}, as a function of the imposed value of k computed for different initial values of k_0 when H = 0.5 m.

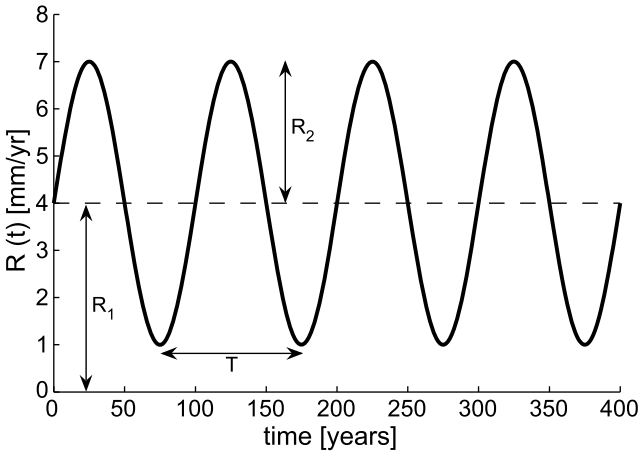

Figure 8. Sketch of the sinusoidal rate of RSLR for a constant rate R_1 = 4 mm yr^{-1}, the amplitude of the oscillations R_2 = 3 mm yr^{-1}, and the period of oscillation T = 100 years.

$$\tau_{SR} = T\left[\frac{1}{4} + \frac{1}{2\pi}\arctan\left(-\frac{Tk}{2\pi H}\right)\right] \tag{14}$$

Equation (13) shows that Q_D varies with the same period as R (see also Figures 9d–9f). We note that H/k has the dimensions of time and can be defined as the "tidal frame filling timescale," T_{FT}; that is, the time required to accrete the marsh platform from MSL to MHT when the maximum accretion rate of a depth equal to H is k. For a given tidal amplitude, T_{FT} decreases with increasing suspended sediment concentration (i.e., marshes in a given tidal setting accrete more rapidly as sediment availability increases), whereas for a given SSC, T_{FT} increases with the tidal amplitude (i.e., for a prescribed sediment supply, marshes in high tidal ranges takes longer to accrete than those in low tidal range settings).

[16] Figure 10a shows that for a given SSC, the ratio between the amplitude of Q_D and R oscillations increases linearly with the period of oscillation (T) for short T values compared to T_{FT}. That is, equation (13) predicts that when $\omega \gg k/H$, the proportionality coefficient of the linear relationship is equal to $k/(2\pi H)$. As T becomes large with respect to T_{FT} (i.e., $\omega \ll k/H$), the amplitude of Q_D oscillations ceases to be a function of T and simply approaches the amplitude of RSLR oscillations. For a given value of T the amplitude of Q_D oscillations increases with increasing SSC (for a fixed tidal range) and decreases with the tidal range (for a constant SSC, see equation (13)). Figure 10b shows that for short T values compared to T_{FT}, time lags increase linearly with the oscillation period ($\tau_{SR} \approx$ T/4), whereas, for larger values of T they reach a constant value. For given values of T and H, τ_{SR} increases as the SSC

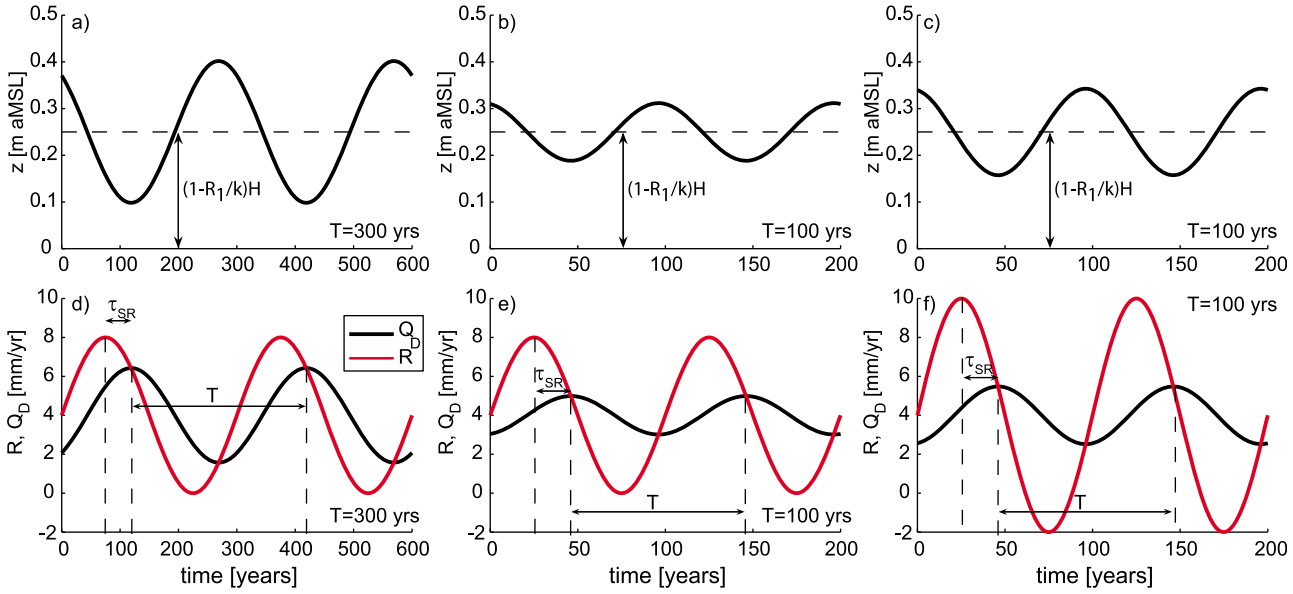

Figure 9. (a–c) Marsh elevations, $z(t)$, and (d–f) related total accretion rates, $Q_D(t)$, when the system is forced with an oscillating rate of RSLR characterized by different periods and amplitudes of oscillation. In Figures 9a and 9d, T = 300 years, R_1 = 4 mm yr^{-1}, and R_2 = 4 mm yr^{-1}. In Figures 9b and 9e, T = 100 years, R_1 = 4 mm yr^{-1}, and R_2 = 4 mm yr^{-1}. In Figures 9c and 9f, T = 100 years, R_1 = 4 mm yr^{-1}, and R_2 = 6 mm yr^{-1}. In all cases we have assumed a sinusoidal tide with amplitude H = 0.5 m, maximum inorganic deposition rate α_T = 5.5 mm yr^{-1}, maximum organic rate γ_0 = 2.5 mm yr^{-1}, and maximum total accretion rate k = 8.0 mm yr^{-1}.

decreases; whereas it increases as the tidal range increases for a fixed SSC (see equation (14)).

3.4. Marsh Response to Accelerating Sea Level Rise

[17] Recent work suggests that sea level rise is accelerating [*Church and White*, 2006; *Jevrejeva et al.*, 2008], and this trend is expected to continue in the coming centuries [e.g., *Rahmstorf*, 2007]. We approximate this trend by considering a steady acceleration of relative sea level rise, where the rate of RSLR evolves through time as $R(t) = R_0 + at$ with R_0 being the initial rate of RSLR and a the acceleration (in dimensions L T^{-2}) in RSLR. Solving equation (7) we find:

$$z(t) = z_0 + \frac{aH}{k}\left[\frac{H}{k}\left(1 - e^{-\frac{k}{H}t}\right) - t\right] \tag{15}$$

$$Q_D(t) = R_0 + a\left[\frac{H}{k}\left(e^{-\frac{k}{H}t}\right) + t\right] \tag{16}$$

If the rate of RSLR steadily increases, marshes will inevitably drown: the marsh will progressively lose elevation with respect to MSL and eventually drown. Using equation (15) we can calculate exactly the time it takes marshes to drown for three different scenarios of accelerating RSLR. Figure 11 shows the time it takes for marshes in different tidal settings (microtidal, mesotidal, and macrotidal) to drown over a range of sediment supply. The *Church and White* [2006] scenario takes their reported acceleration of 20th century sea level rise: 0.008 mm yr^{-2}. Note that this is a conservative estimate; *Church and White* [2006] reported a late 20th century acceleration (a) of 0.013 mm yr^{-2}, and *Jevrejeva et al.* [2008] reported an acceleration of 0.01 mm yr^{-2} since the end of the 18th century. We also fit the IPCC A1B sea level rise scenario; the fit of this scenario results in a = 0.03 mm yr^{-2}. Finally, the *Rahmstorf* [2007] curve is fit resulting a = 0.2 mm yr^{-2}. In all scenarios we take the estimate of the current rate of sea level rise, 1.7 mm yr^{-1} from *Church and White* [2006].

[18] Our results are consistent with the numerical study of *Kirwan et al.* [2010] in that both predict that marsh death under the *Rahmstorf* [2007] sea level rise scenario will occur within a decade of the year 2100 (Figure 11) in the case of a microtidal marsh forced with an SSC C_0 = 30 mg L^{-1}. Our model, however, has the advantage that it allows rapid evaluation of how changing sediment supply can influence the time until marsh drowning. We find that the time a marsh takes to die and therefore to become a tidal flat, t_{death}, increases with increasing sediment availability and tidal amplitude, and decreases as the rate of RSLR accelerates.

4. Discussion

[19] The analytical solutions presented herein allow rapid estimation of the response of salt marshes to variations in physical (e.g., changes in the rate of RSLR and SSC) and biological (e.g., plant productivity) forcings. These solutions also describe the system's behavior over time and its sensitivity to variations in key parameters commonly adopted in recent numerical models of salt marsh evolution [e.g., *Kirwan et al.*, 2010]. The model provides results which agree with those of a number of classical and recent numerical models of salt marsh morphodynamics [e.g., *Allen*, 1990, 1995; *French*, 1993; *Morris et al.*, 2002; *Temmerman et al.*, 2003; *D'Alpaos et al.*, 2007; *Kirwan and*

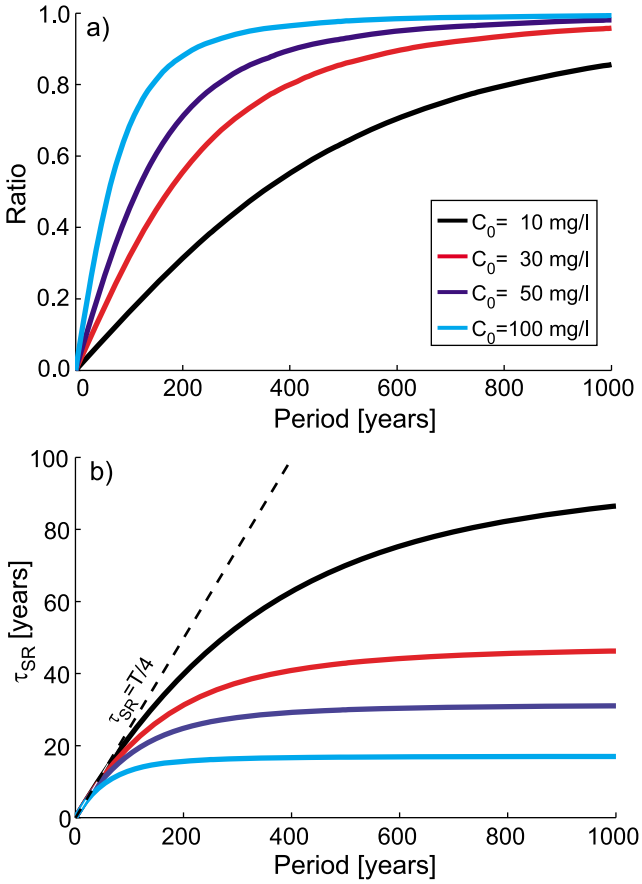

Figure 10. (a) Ratio between the amplitude of Q_D oscillations and the amplitude of RSLR oscillations (R_2) as a function of the period of oscillation, T, for different C_0 values. (b) Time lags, τ_{SR}, as a function of T for different C_0 values. For both Figures 10a and 10b, γ_0 = 2.5 mm yr^{-1} and H = 0.5 m.

Murray, 2007; *Marani et al.*, 2007; *Mudd et al.*, 2009] and bring new insights on recent analyses of marsh response to changing rates of RSLR and sediment supply [e.g., *Marani et al.*, 2007; *Kirwan and Murray*, 2008; *Kirwan et al.*, 2010, 2011; *D'Alpaos*, 2011]. As an example, Figure 12 shows predicted threshold rates of RSLR for marsh drowning as a function of the forcing SSC, for three different tidal ranges (solid lines). When the forcing rate of RSLR exceeds the threshold rate, marshes are likely to be replaced by tidal flats. Our model allows an instantaneous determination of the critical rate of RSLR for marsh survival, as it immediately follows from equation (7) that $R = k$ is the maximum rate of RSLR a marsh can tolerate. As soon as $R > k$, $z < 0$ and the marsh experiences a transition to a tidal flat. Our results compare quite favorably with field observations and with the results obtained by *Kirwan et al.* [2010]. These authors considered five numerical models, designed to analyze salt marsh systems in tidal environments quite different in their tidal, vegetational, and hydrodynamic features, to predict the threshold rates of RSLR responsible for the drowning of marshes characterized by different tidal settings and sediment availability. The predicted threshold rates of RSLR obtained from our analytical model (solid lines in Figure 12) nicely match the best approximation to the average results of the numerical simulations. Moreover our analytical approach accounts for the crucial role exerted by vegetation on marsh stability and resilience. The presence of plants increases the rates of vertical accretion enhancing the resilience of marshes to increasing rates of RSLR (see, e.g., Figure 1). In a hypothetical nonvegetated setting $k_{NV} = \alpha_T$, whereas with vegetation we have $k = \alpha_T + \gamma_0 > k_{NV}$; therefore larger k values allow marshes to keep pace with larger R values. Vegetation growth increases marsh accretion to such an extent that it allows existing marshes to keep pace with R values and SSCs that would preclude salt marsh surfaces from developing in the first

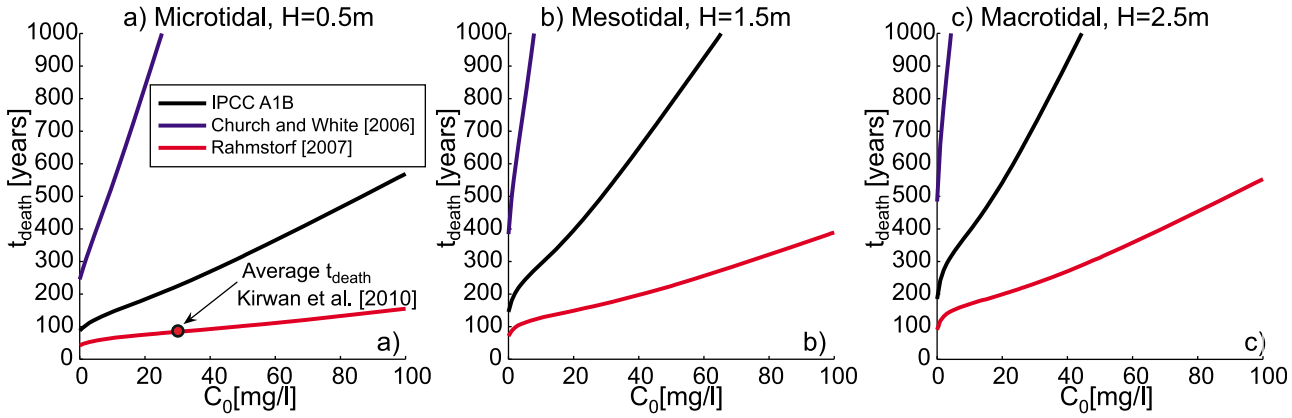

Figure 11. Time a marsh takes to drown and become a tidal flat, t_{death}, as a function of sediment availability for (a) microtidal (H = 0.5 m), (b) mesotidal (H = 1.5 m), and (c) macrotidal marshes (H = 2.5 m). For Figures 11a–11c, γ_0 = 2.5 mm yr^{-1} and C_0 = 30 mg L^{-1} (see Table 1 for the corresponding α_T values). Three different scenarios of acceleration in RMSL are considered, namely a = 0.008 mm yr^{-2} according to *Church and White* [2006] (blue lines), a = 0.03 mm yr^{-2} according to the IPCC A1B sea level rise scenario (black lines), and a = 0.2 mm yr^{-2} according to *Rahmstorf* [2007] (red lines). For a microtidal marsh with SSC C_0 = 30 mg L^{-1} the five models run in the study of *Kirwan et al.* [2010] predicted marsh death ranging from 49 to 105 years, with a mean of 84 years. The time to marsh death predicted by our analytical model exactly matches the mean time of the modeling study: 84 years.

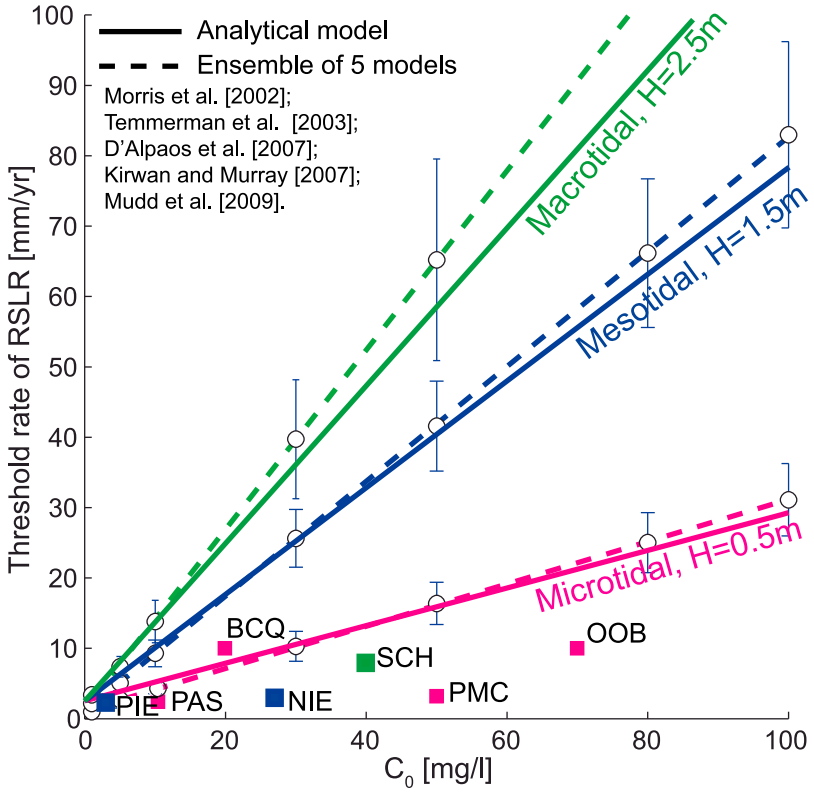

Figure 12. Predicted threshold rate of RSLR, above which marshes experience a transition to a tidal flat. The threshold rate of RSLR (solid lines) is computed as a function of the tidal amplitude and of the SSC (see, e.g., equation (7)). For a given value of H and of the forcing concentration, marshes characterized by rates of RLSR larger than the threshold rate will drown. Dashed lines portray the ensemble of the numerical results of five ecomorphodynamic models of marsh evolution as reported by *Kirwan et al.* [2010] (circles represent the average of the results of the five models for each of the seven considered values of the forcing SSC, whereas the bars represent standard deviation of model results). We have also included examples (denoted by squares) of marshes worldwide characterized by different rates of historical RLSR, sediment concentration, and tidal range (Abbreviations from *Kirwan et al.* [2010] are as follows: PIE, Plum Island Estuary, Massachusetts; PAS, Pamlico Sound, North Carolina; BCQ, Bayou Chitique, Louisiana; NIE, North Inlet Estuary, South Carolina; SCH, Scheldt Estuary, Netherlands; PCM, Phillips Creek Marsh, Virginia; OOB, Old Oyster Bayou, Louisiana).

place, consistent with the numerical results of *D'Alpaos* [2011] and *Kirwan et al.* [2011].

[20] It is also worthwhile observing that the predicted time it takes for marshes in microtidal settings (1 m tidal range) to drown when forced with an SSC $C_0 = 30$ mg L^{-1} and the *Rahmstorf* [2007] sea level rise scenario (Figure 11) is nearly identical to average time predicted by the five numerical models described in the work of *Kirwan et al.* [2010] (the average t_{death} is of about 84 years, with maximum and minimum values of about 49 and 105 years, respectively).

[21] It is therefore worth emphasizing that our analyses do not require long numerical simulations because our model describes the full impact of a range of changing external forcings within a small number of analytical solutions. In contrast, to analyze the effects of a sinusoidal rate of RSLR, *Allen* [1995] carried out more than 110 numerical simulations which allowed him to explore the role of sediment supply, vegetation productivity, oscillation period of the rate of RSLR and amplitude of the oscillation, without considering the role of the tidal range. Numerical models can be computationally expensive; owing to computational expense a full exploration of marsh response to changing sea level rise and sediment supply, or to variations in the quantities representative of the processes involved, has been difficult [e.g., *Allen*, 1995; *Kirwan and Murray*, 2008; *D'Alpaos*, 2011].

[22] In agreement with *Kirwan and Murray* [2008], we find that in the case of a sinusoidal rate of RSLR, increasing the period of oscillation may have little effect on the time lag (see Figure 10b). However, we observe that this is true only as long as the oscillation period is larger than the "tidal frame filling timescale"; that is, $T > T_{FT}$. For a tidal amplitude $H = 0.5$ m and large sediment supply ($C_0 = 100$ mg L^{-1}), $T_{FT} \sim 17$ years, and τ_{SR} increases from 13 to 17 years as T increases from 100 to 500 years. However, we also observe that as the SSC decreases (e.g., $C_0 = 10$ mg L^{-1}), time lags are strongly affected by the period of sea level oscillations: $T_{FT} \sim 96$ years (for $H = 0.5$ m) and τ_{SR} increases from 22 to 70 years as T increases from 100 to 500 years. From equation (14) it emerges that the time lag τ_{SR} depends on sediment availability, tidal range, and RSLR oscillation

period, whereas it is independent of the amplitude of RSLR oscillations: increasing the amplitude of oscillation has no effect on lag time. When the period of oscillation is short, the lag between sea level oscillations and marsh accretion (τ_{SR}) reduces to $T/4$ (Figure 10b). *Kolker et al.* [2009] report both accretion rates and the rate of sea level rise for a number of cores in the Long Island region near New York. Their data show the rate of sea level rise varying on short (~4–12 years) timescales; thus in this environment our model predict a very short (1–4 years) lag, consistent with *Kolker et al.* [2009]. Our model, however, predicts that the oscillations will be severely damped. *Kolker et al.* [2009] do not report suspended sediment concentrations but, on the basis of typical suspended sediment concentrations of 30–100 mg L^{-1} and their reported bulk density of 0.2–0.4 g cm^{-3}, our model predicts that accretion rates should oscillate with an amplitude that is <10% of the amplitude of oscillations in the rate of sea level rise. This too, is consistent with *Kolker et al.* [2009, Figure 6] (note the difference in scale in their reported rate of SLR versus accretion rate).

[23] The ratio between the amplitude of Q_D and RSLR oscillations increases with T but it is strongly related to sediment availability and tidal range, whose effect is accounted for in T_{FT} (Figure 10a). Equation (13), in fact, shows that the amplitude of Q_D oscillations depends on sediment availability, tidal range, RSLR oscillation period, and amplitude. Because the amplitude of Q_D oscillations depends on the value of the oscillation period, T, relative to the filling timescale, T_{FT}, our results suggest that marsh stratigraphy will be unable to fully record short-term fluctuations in MSL which could be captured only if $T \gg T_{FT}$ (i.e., $\omega \ll k/H$), in agreement with numerical modeling [*Kirwan and Murray*, 2008]. The shortest T_{FT} values are of 15 years for $H = 0.25$ m and $C_0 = 100$ mg L^{-1} (i.e., in the case of microtidal settings with quite large maximum sedimentation; see Table 1). Therefore annual RSLR oscillations cannot be captured by stratigraphic analyses (i.e., only 1% of annual RSLR oscillations will be captured in marsh stratigraphy in this case). As to the long-term fluctuations in R, the sedimentation rate will be a very damped version of the historical rate of RSLR in macrotidal settings characterized by low SSCs (i.e., with large T_{FT} values). Our results suggest that marsh cores can be used to determine long-term fluctuations in MSL in agreement with previous modeling approaches [e.g., *Allen*, 1995; *Kirwan and Murray*, 2008] but emphasize that this technique will be most effective in sediment rich, microtidal settings.

[24] Our model also supports the long-standing paradigm that marsh stability is positively correlated with tidal amplitude [e.g., *Kirwan and Guntenspergen*, 2010]. The maximum constant rate of RSLR a marsh can survive, in fact, is equal to k, which increases with sediment availability and tidal range (see, e.g., Table 1 and Figure 2). Moreover, the time a marsh requires to adjust to a newly imposed constant rate of RSLR increases as H increases (Figure 5), showing that marshes with low tidal ranges respond more quickly to changes in the forcings. If the rate of RSLR varies sinusoidally, marshes in high tidal range settings can survive higher rates of RSLR (equations (13) and (14)) and for fixed characteristics of the sinusoidal forcing (period T and amplitude R_2) and a given SSC, time lags increase with the tidal range (see equation (14)), whereas the ability of marsh accretion rates to mimic the amplitude of RSLR oscillations decreases as the tidal range increases. This means that marshes in high tidal range settings respond more slowly to MSL fluctuations than microtidal marshes, and that these marshes are less likely to record long-term MSL fluctuations in their marsh stratigraphy.

[25] We observe that marshes are more resilient to a step decrease in the rate of RSLR rather than to a step increase: the time required to match new equilibrium configurations in the case of a step increase in R is shorter than in the case of a step decrease (of the same amount) in R. Figure 6 shows that a marsh takes about 160 years to reach equilibrium with a rate of RSLR equal to 6 mm yr^{-1}, starting from $R_0 = 2$ mm yr^{-1}, whereas it takes more than 230 years to go back to an elevation in equilibrium with $R = 2$ mm yr^{-1}. This result has important consequences because even if the current rate of RSLR was reduced to values typical of the past, marshes would require longer to equilibrate than it took in the past to equilibrate to the occurred increase in R. Our results suggest that marshes will adapt (or drown, depending on forcings) faster to future rates of RSLR than they did in the past. If it took about 145 years for a marsh (with k = 8.0 mm yr^{-1} and H = 0.5 m) to adapt to a rate R = 4 mm yr^{-1}, starting from a rate $R_0 = 2$ mm yr^{-1}, it will take less time (119 years) to adapt to a rate $R = 6$ mm yr^{-1}, starting from a rate $R_0 = 4$ mm yr^{-1}.

[26] However, marshes respond more rapidly to an increase in sediment load or vegetation productivity than to a decrease (of the same amount) in sediment load or vegetation productivity (Figure 7). This means that if management decisions resulting in increased sediment loads are taken, marshes will adapt more rapidly to new equilibrium conditions than they did in the past when sediment availability was reduced. Land managers concerned about the viability of their marshes may be encouraged by this result since local measures, over which they may have direct control (i.e., increasing sediment supply by enhancing the amount of sediment flushed from upstream dams) are more effective at buffering marshes against environmental change than global measures (e.g., global policies that reduce eustatic sea level rise). The model also demonstrates that the deleterious effects of rising sea level, specifically the drowning of marshes and their conversion to mudflats, can be counteracted via informed management of sediment supply. Our model allows rapid estimation of the additional sediment needed to counteract threats to marsh stability under future RSLR scenarios without resorting to time consuming numerical modeling. Managers should, however, be aware of the limitations of the approach as the model only addresses the average elevation of a marsh platform. Because sediment concentrations vary as a function of position on the marsh [e.g., *Christiansen et al.*, 2000] its response to changing RSLR will also be spatially varied [e.g., *D'Alpaos*, 2011]. Moreover, we have considered a marsh populated by a single vegetation species, namely *Spartina alterniflora*, and have condensed in the parameters α_T and γ_O the characteristics of such species [*Morris and Haskin*, 1990]. Vegetation dynamics over the platform and the nonlinearities in the accretion rates related to the geomorphic structure of the salt marsh and of the channel network cutting through it, and to vegetation patches, have not been considered in our spatially averaged

approach. The description of sediment transport and vegetation dynamics over the platform, in fact, requires the use of nonspatially averaged models [e.g., *Mudd et al.*, 2004; *D'Alpaos et al.*, 2007; *Temmerman et al.*, 2007]. In addition we do not consider the evolution of the marsh boundary: our model could predict a stabile marsh but this marsh may still be susceptible to destruction via wave erosion at its boundary [e.g., *Mariotti et al.*, 2010].

5. Conclusions

[27] We have provided a simple analytical representation of salt marsh dynamics in response to changes in external forcings such as suspended sediment concentration and the rate of relative sea level rise. Our parsimonious analytical model, despite containing simplifying assumptions, retains the key biogeomorphic processes governing the vertical evolution of salt marsh ecosystems. Model results are consistent with field observations and with results of previous numerical models, but do not require long numerical simulations. Our model describes the full impact of a range of changing external forcings within a small number of analytical solutions furthermore providing means to improve our understanding of salt marsh biomorphodynamics. The main conclusions of this paper are:

[28] 1. In the case of a constant rate of RSLR, threshold rates for marsh drowning, obtained through our model, are consistent with those determined through more sophisticated and computationally expensive biomorphodynamic models of marsh evolution. In particular we observe that for a given SSC the threshold rate of RSLR responsible for marsh drowning is greater in marshes with greater tidal amplitudes.

[29] 2. Marshes are more resilient to a step decrease in the rate of relative sea level rise rather than to a step increase of the same magnitude. However, marshes respond more rapidly to an increase in sediment load or vegetation productivity, rather than to a decrease (of the same amount) in sediment load or vegetation productivity. This is of critical importance for land managers concerned about the long-term viability of salt marshes in response to anthropogenic disturbance.

[30] 3. Sediment rich or highly productive marshes respond faster to environmental perturbation, and this effect is more pronounced for marshes in high tidal ranges. Marsh stability is therefore positively correlated with tidal amplitude: marshes with high tidal ranges respond more slowly to changes in the environmental forcings and therefore are less likely to be affected by perturbations.

[31] 4. In the case of a sinusoidal rate of RSLR, the total accretion rate, Q_D, oscillates around its average value with a reduced amplitude compared to that of the oscillating rate of RSLR, and a lag is observed between maximum accretion rates and maximum rates of RSLR. As long as the oscillation period T is smaller than the "tidal frame filling timescale" T_{FT}, both the amplitude of Q_D oscillations and the lag τ_{SR} depend on sediment availability, tidal range, RSLR oscillation period, whereas the amplitude of Q_D oscillations is also a function of the amplitude of RSLR oscillations. However, when $T > T_{FT}$ both quantities become independent of T tending toward a constant value which depends on sediment availability and tidal range. Marsh stratigraphy will be unable to fully record short-term fluctuations in RMSL, whereas it will be able to capture long-term fluctuations particularly in sediment rich, microtidal settings.

[32] 5. The model predicts the time to marsh drowning under a scenario in which sea level accelerates; such an acceleration has been observed over the 20th century [e.g., *Church and White*, 2006] and is predicted to continue in the future [e.g., *Rahmstorf*, 2007]. Our model predicts that if the acceleration in SLR maintains its late 20th century trend, marshes with SSC > 20 mg L^{-1} will be viable for at least a millennium, whereas under the *Rahmstorf* [2007] scenario some marshes will drown in this century. These predictions could be used by coastal managers to aid in decision making about regulating sediment supply in order to maintain the viability of coastal marshes.

[33] **Acknowledgments.** This work was supported by the 2008 University of Padua project "Valutazione delle condizioni di stabilità di argini fluviali tramite modellazione matematica e indagini non invasive" and by Comune di Venezia "Modificazioni morfologiche della laguna, perdita e reintroduzione dei sedimenti." We thank the Editor, Associate Editor, Matt Kirwan, Laurel Larsen, and one anonymous reviewer for their helpful comments and suggestions.

References

Allen, J. R. L. (1990), Salt-marsh growth and stratification: A numerical model with special reference to the Severn Estuary, southwest Britain, *Mar. Geol.*, *95*, 77–96, doi:10.1016/0025-3227(90)90042-I.

Allen, J. R. L. (1995), Salt-marsh growth and fluctuating sea level: Implications of a simulation model for Flandrian coastal stratigraphy and peat-based sea-level curves, *Sediment. Geol.*, *100*, 21–45, doi:10.1016/0037-0738(95)00101-8.

Augustin, L. N., J. L. Irish, and P. Lynett (2009), Laboratory and numerical studies of wave damping by emergent and near-emergent wetland vegetation, *Coastal Eng.*, *56*, 332–340, doi:10.1016/j.coastaleng.2008.09.004.

Blum, M. D., and H. H. Roberts (2009), Drowning of the Mississippi Delta due to insufficient sediment supply and global sea-level rise, *Nat. Geosci.*, *2*, 488–491, doi:10.1038/ngeo553.

Carniello, L., A. Defina, S. Fagherazzi, and L. D'Alpaos (2005), A combined wind wave–tidal model for the Venice lagoon, Italy, *J. Geophys. Res.*, *110*, F04007, doi:10.1029/2004JF000232.

Chmura, G. L., S. C. Anisfeld, D. R. Cahoon, and J. C. Lynch (2003), Global carbon sequestration in tidal, saline wetland soils, *Global Biogeochem. Cycles*, *17*(4), 1111, doi:10.1029/2002GB001917.

Christiansen, T., P. L. Wiberg, and T. G. Milligan (2000), Flow and sediment transport on a tidal salt marsh surface, *Estuarine Coastal Shelf Sci.*, *50*, 315–331, doi:10.1006/ecss.2000.0548.

Church, J., and N. White (2006), A 20th century acceleration in global sea level rise, *Geophys. Res. Lett.*, *33*, L01602, doi:10.1029/2005GL024826.

Costanza, R., et al. (1997), The value of the world's ecosystem services and natural capital, *Nature*, *387*, 253–260, doi:10.1038/387253a0.

D'Alpaos, A. (2011), The mutual influence of biotic and abiotic components on the long-term ecomorphodynamic evolution of salt-marsh ecosystems, *Geomorphology*, *126*, 269–278, doi:10.1016/j.geomorph.2010.04.027.

D'Alpaos, A., S. Lanzoni, S. M. Mudd, and S. Fagherazzi (2006), Modelling the influence of hydroperiod and vegetation on the cross-sectional formation of tidal channels, *Estuarine Coastal Shelf Sci.*, *69*, 311–324, doi:10.1016/j.ecss.2006.05.002.

D'Alpaos, A., S. Lanzoni, M. Marani, and A. Rinaldo (2007), Landscape evolution in tidal embayments: Modeling the interplay of erosion, sedimentation, and vegetation dynamics, *J. Geophys. Res.*, *112*, F01008, doi:10.1029/2006JF000537.

Day, J. W., J. Rybczyk, F. Scarton, A. Rismondo, D. Are, and G. Cecconi (1999), Site accretionary dynamics, sea-level rise and the survival of wetlands in Venice lagoon: A field and modelling approach, *Estuarine Coastal Shelf Sci.*, *49*, 607–628, doi:10.1006/ecss.1999.0522.

Day, J. W., G. P. Shaffer, L. D. Britsch, D. J. Reed, S. R. Hawes, and D. Cahoon (2000), Pattern and process of land loss in the Mississippi Delta: A spatial and temporal analysis of wetland habitat change, *Estuaries*, *23*, 425–438, doi:10.2307/1353136.

Fagherazzi, S., L. Carniello, L. D'Alpaos, and A. Defina (2006), Critical bifurcation of shallow microtidal landforms in tidal flats and salt marshes, *Proc. Natl. Acad. Sci. U. S. A.*, *103*, 8337–8341, doi:10.1073/pnas.0508379103.

French, J. R. (1993), Numerical simulation of vertical marsh growth and adjustment to accelerated sea-level rise, north Norfolk, UK, *Earth Surf. Processes Landforms*, *18*, 63–81, doi:10.1002/esp.3290180105.

Howes, N. C., D. M. FitzGerald, Z. J. Hughes, I. Y. Georgiou, M. A. Kulp, M. D. Miner, J. M. Smith, and J. A. Barras (2010), Hurricane-induced failure of low salinity wetlands, *Proc. Natl. Acad. Sci. U. S. A.*, *107*, 14,014–14,019, doi:10.1073/pnas.0914582107.

Jevrejeva, S., J. Moore, A. Grinsted, and P. Woodworth (2008), Recent global sea level acceleration started over 200 years ago?, *Geophys. Res. Lett.*, *35*, L08715, doi:10.1029/2008GL033611.

Kirwan, M. L., and G. R. Guntenspergen (2010), Influence of tidal range on the stability of coastal marshland, *J. Geophys. Res.*, *115*, F02009, doi:10.1029/2009JF001400.

Kirwan, M. L., and A. B. Murray (2007), A coupled geomorphic and ecological model of tidal marsh evolution, *Proc. Natl. Acad. Sci. U. S. A.*, *104*, 6118–6122, doi:10.1073/pnas.0700958104.

Kirwan, M. L., and A. B. Murray (2008), Tidal marshes as disequilibrium landscapes? Lags between morphology and Holocene sea level change, *Geophys. Res. Lett.*, *35*, L24401, doi:10.1029/2008GL036050.

Kirwan, M. L., G. R. Guntenspergen, A. D'Alpaos, J. T. Morris, S. M. Mudd, and S. Temmerman (2010), Limits on the adaptability of coastal marshes to rising sea level, *Geophys. Res. Lett.*, *37*, L23401, doi:10.1029/2010GL045489.

Kirwan, M. L., A. B. Murray, J. P. Donnelly, and D. R. Corbett (2011), Rapid wetland expansion during European settlement and its implication for marsh survival under modern sediment delivery rates, *Geology*, *39*, 507–510, doi:10.1130/G31789.1.

Kolker, A. S., S. L. Goodbred, S. Hameed, and J. K. Cochran (2009), High resolution records of coastal systems responses to short-term sea level variability, *Estuarine Coastal Shelf Sci.*, *84*, 493–508, doi:10.1016/j.ecss.2009.06.030.

Krone, R. B. (1987), A method for simulating historic marsh elevations, in *Coastal Sediments '87*, edited by N. C. Krause, pp. 316–323, Am. Soc. Civ. Eng., New York.

Larsen, L. G., and J. W. Harvey (2010), How vegetation and sediment transport feedbacks drive landscape change in the Everglades and wetlands worldwide, *Am. Nat.*, *176*, E66–E79, doi:10.1086/655215.

Larsen, L. G., S. Moseman, A. E. Santoro, K. Hopfensperger, and A. Burgin (2010), A complex-systems approach to predicting effects of sea level rise and nitrogen loading on nitrogen cycling in coastal wetland ecosystems, in *Eco-DAS VIII Symposium Proceedings*, edited by P. F. Kemp, pp. 67–92, Assoc. for the Sci. of Limnol. and Oceanogr., Waco, Tex.

Li, H., and S. L. Yang (2009), Trapping effect of tidal marsh vegetation on suspended sediment, Yangtze Delta, *J. Coastal Res.*, *25*, 915–924, doi:10.2112/08-1010.1.

Marani, M., S. Lanzoni, S. Silvestri, and A. Rinaldo (2004), Tidal landforms, patterns of halophytic vegetation and the fate of the lagoon of Venice, *J. Mar. Syst.*, *51*, 191–210, doi:10.1016/j.jmarsys.2004.05.012.

Marani, M., A. D'Alpaos, S. Lanzoni, L. Carniello, and A. Rinaldo (2007), Biologically controlled multiple equilibria of tidal landforms and the fate of the Venice lagoon, *Geophys. Res. Lett.*, *34*, L11402, doi:10.1029/2007GL030178.

Marani, M., A. D'Alpaos, S. Lanzoni, L. Carniello, and A. Rinaldo (2010), The importance of being coupled: Stable states and catastrophic shifts in tidal biomorphodynamics, *J. Geophys. Res.*, *115*, F04004, doi:10.1029/2009JF001600.

Mariotti, G., S. Fagherazzi, P. L. Wiberg, K. J. McGlathery, L. Carniello, and A. Defina (2010), Influence of storm surges and sea level on shallow tidal basin erosive processes, *J. Geophys. Res.*, *115*, C11012, doi:10.1029/2009JC005892.

McKee, K. L., and W. H. Patrick (1988), The relationship of smooth cordgrass (*Spartina alterniflora*) to tidal datums—A review, *Estuaries*, *11*, 143–151, doi:10.2307/1351966.

Möller, I., T. Spencer, J. R. French, D. Leggett, and M. Dixon (1999), Wave transformation over salt marshes: A field and numerical modelling study from North Norfolk, England, *Estuarine Coastal Shelf Sci.*, *49*, 411–426, doi:10.1006/ecss.1999.0509.

Morris, J. T., and B. Haskin (1990), A 5-yr record of aerial primary production and stand characteristics of *Spartina alterniflora*, *Ecology*, *71*, 2209–2217, doi:10.2307/1938633.

Morris, J. T., P. V. Sundareshwar, C. T. Nietch, B. Kjerfve, and D. R. Cahoon (2002), Responses of coastal wetlands to rising sea level, *Ecology*, *83*, 2869–2877, doi:10.1890/0012-9658(2002)083[2869:ROCWTR]2.0.CO;2.

Mudd, S. M. (2011), The life and death of salt marshes in response to anthropogenic disturbance of sediment supply, *Geology*, *39*, 511–512, doi:10.1130/focus052011.1.

Mudd, S. M., S. Fagherazzi, J. T. Morris, and D. J. Furbish (2004), Flow, sedimentation, and biomass production on a vegetated salt marsh in South Carolina: Toward a predictive model of marsh morphologic and ecologic evolution, in *The Ecogeomorphology of Salt Marshes, Coastal Estuarine Sci.*, vol. 59, edited by S. Fagherazzi, M. Marani, and L. K. Blum, pp. 165–188, AGU, Washington, D. C.

Mudd, S. M., S. Howell, and J. T. Morris (2009), Impact of dynamic feedbacks between sedimentation, sea-level rise, and biomass production on near surface marsh stratigraphy and carbon accumulation, *Estuarine Coastal Shelf Sci.*, *82*, 377–389, doi:10.1016/j.ecss.2009.01.028.

Mudd, S. M., A. D'Alpaos, and J. T. Morris (2010), How does vegetation affect sedimentation on tidal marshes? Investigating particle capture and hydrodynamic controls on biologically mediated sedimentation, *J. Geophys. Res.*, *115*, F03029, doi:10.1029/2009JF001566.

Neubauer, S. C. (2008), Contributions of mineral and organic components to tidal freshwater marsh accretion, *Estuarine Coastal Shelf Sci.*, *78*, 78–88, doi:10.1016/j.ecss.2007.11.011.

Neumeier, U., and P. Ciavola (2004), Flow resistance and associated sedimentary processes in a *Spartina maritima* salt marsh, *J. Coastal Res.*, *20*, 434–447.

Nyman, J. A., R. J. Walters, R. D. Delaune, and W. H. Patrick (2006), Marsh vertical accretion via vegetative growth, *Estuarine Coastal Shelf Sci.*, *69*, 370–380, doi:10.1016/j.ecss.2006.05.041.

Perillo, G. M. E., E. Wolanski, D. Cahoon, and M. Brinson (Eds.) (2009), *Coastal Wetlands: An Integrated Ecosystem Approach*, Elsevier, Burlington, Vt.

Rahmstorf, S. (2007), A semi-empirical approach to projecting future sea-level rise, *Science*, *315*, 368–370, doi:10.1126/science.1135456.

Randerson, P. F. (1979), A simulation model of salt-marsh development and plant ecology, in *Estuarine and Coastal Land Reclamation and Water Storage*, edited by B. Knights and A. J. Phillips, pp. 48–67, Saxon House, Farnborough, U. K.

Rybczyk, J. M., and D. R. Cahoon (2002), Estimating the potential for submergence for two wetlands in the Mississippi River Delta, *Estuaries*, *25*, 985–998, doi:10.1007/BF02691346.

Silvestri, S., A. Defina, and M. Marani (2005), Tidal regime, salinity and salt marsh plant zonation, *Estuarine Coastal Shelf Sci.*, *62*, 119–130, doi:10.1016/j.ecss.2004.08.010.

Temmerman, S., G. Govers, P. Meire, and S. Wartel (2003), Modelling long-term tidal marsh growth under changing tidal conditions and suspended sediment concentrations, Scheldt estuary, Belgium, *Mar. Geol.*, *193*, 151–169, doi:10.1016/S0025-3227(02)00642-4.

Temmerman, S., T. J. Bouma, J. Van de Koppel, D. Van der Wal, M. B. De Vries, and P. M. J. Herman (2007), Vegetation causes channel erosion in a tidal landscape, *Geology*, *35*, 631–634, doi:10.1130/G23502A.1.

A. D'Alpaos, Department of Geosciences, University of Padova, Via Gradenigo 6, Padua I-35131, Italy. (andrea.dalpaos@unipd.it)

L. Carniello, Department IMAGE, University of Padova, Via Loredan 20, Padua I-35131, Italy. (carniello@idra.unipd.it)

S. M. Mudd, School of GeoSciences, University of Edinburgh, Drummond Street, Edinburgh EH8 9XP, UK. (simon.m.mudd@ed.ac.uk)